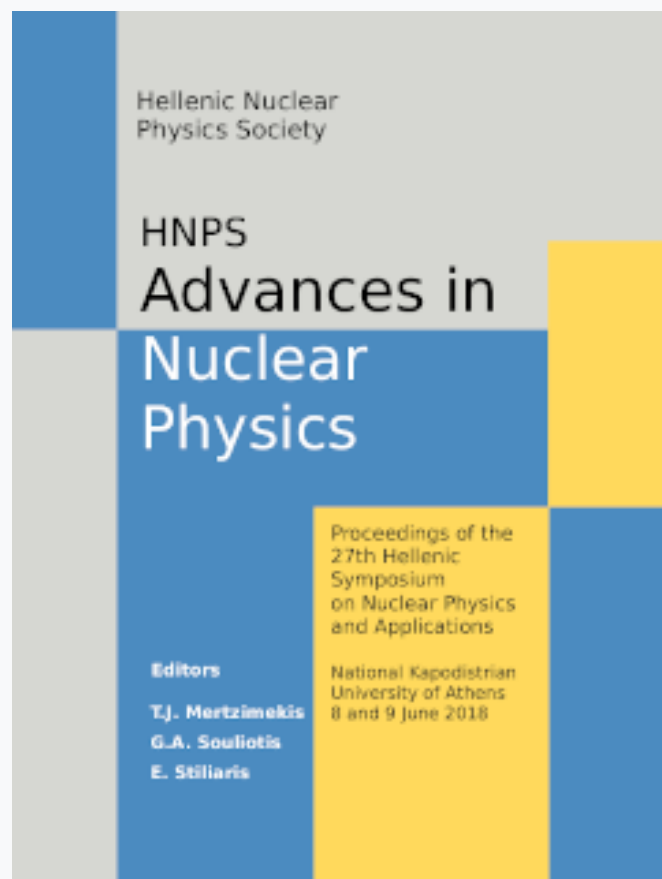


## Annual Symposium of the Hellenic Nuclear Physics Society

Τόμ. 26 (2018)

HNPS2018



**Study of the  $^{234,236}\text{U}(\text{n},\text{f})$  and  $^{232}\text{Th}(\text{n},\text{f})$  cross sections in the energy range between 14.8 and 19.2 MeV with Micromegas detectors**

*S. Chasapoglou, V. Michalopoulou, A. Stamatopoulos, A. Kalamara, M. Kokkoris, R. Vlastou, A. Lagoyannis, Z. Eleme, N. Patronis*

doi: [10.12681/hnps.1826](https://doi.org/10.12681/hnps.1826)

### Βιβλιογραφική αναφορά:

Chasapoglou, S., Michalopoulou, V., Stamatopoulos, A., Kalamara, A., Kokkoris, M., Vlastou, R., Lagoyannis, A., Eleme, Z., & Patronis, N. (2019). Study of the  $^{234,236}\text{U}(\text{n},\text{f})$  and  $^{232}\text{Th}(\text{n},\text{f})$  cross sections in the energy range between 14.8 and 19.2 MeV with Micromegas detectors. *Annual Symposium of the Hellenic Nuclear Physics Society*, 26, 230–234. <https://doi.org/10.12681/hnps.1826>

# Study of the $^{234,236}\text{U}(\text{n},\text{f})$ and $^{232}\text{Th}(\text{n},\text{f})$ cross sections in the energy range between 14.8 and 19.2 MeV with Micromegas detectors

S. Chasapoglou<sup>1</sup>, V. Michalopoulou<sup>1,2</sup>, A. Stamatopoulos<sup>1</sup>, A. Kalamara<sup>1</sup>, M. Kokkoris<sup>1</sup>, R. Vlastou<sup>1</sup>, A. Lagoyannis<sup>3</sup>, Z. Eleme<sup>4</sup>, N. Patronis<sup>4</sup>

<sup>1</sup> Department of Physics, National Technical University of Athens, Zografou Campus, 15780 Athens, Greece

<sup>2</sup> European Organization of Nuclear Research (CERN), Geneva, Switzerland

<sup>3</sup> Tandem Accelerator Laboratory, Institute of Nuclear Physics, N.C.S.R. "Demokritos", Aghia Paraskevi, 15310 Athens, Greece

<sup>4</sup> Department of Physics, University of Ioannina, 45110 Ioannina, Greece

**Abstract** The design of fast nuclear reactors and accelerator driven systems is very strongly based on the accurate knowledge of neutron-induced fission cross sections on several actinides, such as  $^{234,236}\text{U}$  and  $^{232}\text{Th}$ . Specifically, these isotopes play an important role in the thorium cycle. Regarding  $(\text{n},\text{f})$  reactions on these isotopes (namely  $^{234,236}\text{U}(\text{n},\text{f})$ ), few available discrepant cross-section datasets exist in literature in the energy range between 14-20 MeV, accompanied by relatively large errors, resulting to poor evaluations. In the present work, the study of the fission cross sections of the  $^{234,236}\text{U}$  and  $^{232}\text{Th}$  was possible with the use of quasi-monoenergetic neutron beams at 14.8, 15.2, 17.8 and 19.2 MeV at the 5.5 MV Tandem Van de Graaff accelerator of NCSR "Demokritos", produced via the  $^3\text{H}(\text{d},\text{n})^4\text{He}$  reaction. Moreover, a methodology is presented for the estimation of the parasitic neutrons present in the experimental area, for facilities with no complementary time-of-flight installation.

**Keywords** fission, parasitic neutrons, quasi-monoenergetic neutron beams

## INTRODUCTION

The study of neutron induced fission cross section on actinides is of great importance for the design of new generation fast nuclear reactors and accelerator driven systems, as well as for the investigation of the mechanism of fission process. More specifically, both  $^{234}\text{U}$  and  $^{236}\text{U}$  play an important role in the thorium fuel cycle, and thus the  $(\text{n},\text{f})$  cross-sections are required with adequate accuracy. However, in the energy range between 14 and 20 MeV, few available discrepant datasets exist in literature [1-8], leading to considerable discrepancies among the latest evaluations [9-11]. More specifically, above 15 MeV the differences among the existing experimental datasets reach up to 13 and 23%, while the relative errors are up to 11 and 8%, for the  $^{234}\text{U}(\text{n},\text{f})$  and  $^{232}\text{Th}(\text{n},\text{f})$  reactions, respectively. On the other hand, for the  $^{236}\text{U}(\text{n},\text{f})$  reaction only one experimental dataset exists in literature [1]. Therefore, there is a need for additional measurements in the above mentioned energy range, implementing different techniques in order to improve the existing evaluations.

In the present work, fission cross section measurements on  $^{234,236}\text{U}$  and  $^{232}\text{Th}$  have been measured at 14.8, 15.2, 17.8 and 19.2 MeV, using Micromegas detectors. The neutron beam was produced via the  $^3\text{H}(\text{d},\text{n})^4\text{He}$  reaction and the main beam is accompanied by low energy parasitic neutrons produced mainly from deuteron-induced reactions with the materials of the

beam line. The contribution of these parasitic neutrons to the fission products have to be subtracted from the experimental counts. A methodology has been developed to encounter this problem, with the use of  $^{238}\text{U}(\text{n},\text{f})$   $^{235}\text{U}(\text{n},\text{f})$  reference reactions, combined with Monte Carlo simulations, as well as with the multiple foil activation technique [13,14].

## EXPERIMENTAL DETAILS

The experiment was performed at the 5.5 MV Tandem Van de Graaf accelerator of the National Center for Scientific Research “Demokritos”. The production of the quasi-monoenergetic neutron beams in the energy range between 14.8 and 19.2 MeV was achieved via the  $^3\text{H}(\text{d},\text{n})^4\text{He}$  reaction, with a Q-value of 17.6 MeV, by bombarding a solid TiT target with deuteron beams. At forward angles this reaction can produce highly energetic neutrons compared to the respective deuteron energy ( $E_d$ ) required. The fluctuations of the neutron beam were monitored with a  $\text{BF}_3$  detector. However, in facilities with no complementary time-of-flight installation for the adequate characterization of the neutron beam, the parasitic neutrons become a problem for fission measurements, since fission cross sections have low thresholds.

The experimental setup consisted of a fission chamber and a holder with the activation foils placed between the tritiated titanium target and the fission chamber (Fig. 1). A liquid scintillator was also used with its axis aligned with the neutron beam at a distance of about 3 m from the fission chamber.

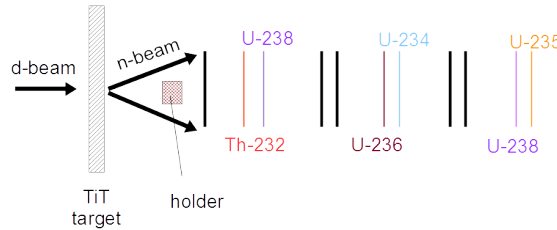


**Fig. 1.** Schematic view of the experimental setup. Black vertical lines represent the Micromegas detectors, while the grey ones represent the actinide targets.

The fission chamber contained six actinide targets along with the Micromegas detectors and it was filled with a mixture of 90% Ar and 10%  $\text{CO}_2$  in atmospheric pressure. The fission fragments produced from the actinide samples were detected with the Micromegas detectors, while the activated foils were measured after the end of the irradiations using HPGe detectors. The  $^{236}\text{U}$  and the  $^{234}\text{U}$  targets were placed back-to-back, to achieve the same neutron flux in both targets. The cross-sections will be deduced relative to the reference cross-section of  $^{238}\text{U}$  and  $^{235}\text{U}$ . The  $^{235}\text{U}$  target was used as a sensitive tool, to low energy neutron background, since the  $^{235}\text{U}(\text{n},\text{f})$  cross-section is notably high in the low energy region.

A typical fission spectrum is presented in Fig. 2, from which the experimental fission fragment yield will be deduced. The  $\alpha$ -background, originating from the radioactivity of the actinide targets and fission fragment regions are evident, with the energy deposition of the  $\alpha$ -particles within the gas volume being smaller relative to the respective deposition of the fission fragments. Some fission fragments though, deposit a lower amount of energy, comparable to the energy of the  $\alpha$ -particles and therefore are lost under the  $\alpha$ -background. An amplitude threshold is then introduced in the analysis for the discrimination of the fission fragments and the  $\alpha$ -background, while the lost counts can be estimated by means of Monte Carlo simulations.

Finally, a further test for estimation of the parasitic neutrons has been tried. A Cu foil was placed in the flange in front of the tritiated target, for every neutron beam energy to prevent the deuteron nuclei from reaching tritium. Thus, any neutron inducing fission events should result from parasitic reactions in the beam line and not from the designated neutron source and should thus be subtracted from the experimental fission yield, after normalization to the same incident deuteron current.

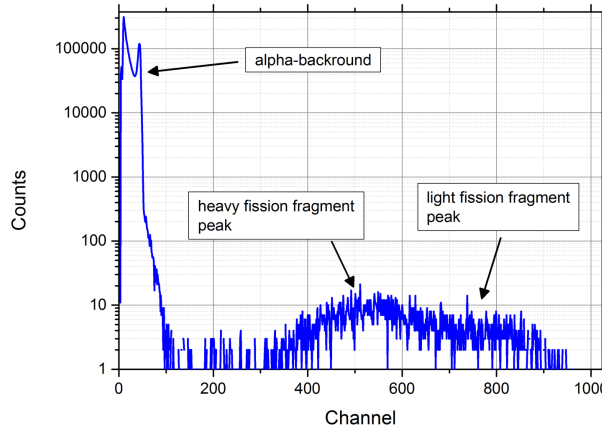


**Fig. 2.**  $^{235}\text{U}$  experimental fission spectrum obtained at  $E_n=16.5$  MeV

## ANALYSIS

The neutron induced fission cross section of the  $^{234}\text{U}(\text{n},\text{f})$ ,  $^{236}\text{U}(\text{n},\text{f})$  and  $^{232}\text{Th}(\text{n},\text{f})$  with respect to  $^{238}\text{U}$ , will be calculated via the formula

$$\sigma(E) = \frac{Y(E)}{Y'(E)} \frac{N'}{N} \frac{\Phi'(E)}{\Phi(E)} \sigma'(E) \quad (1)$$

Where

- $Y$  is the experimental fission yield recorded in the Micromegas detector for each of the actinide targets, that will be corrected for the amplitude cut introduced in the analysis and any parasitic contribution from low energy neutrons.
- $N$  is the total number of atoms of the target in question
- $\Phi$  is the neutron fluence on each target
- $\sigma'$  the cross section of the  $^{238}\text{U}(\text{n},\text{f})$  reference reaction

Every tilted variable refers to  $^{238}\text{U}$  reference target.

The data analysis is still in progress, since the effect of parasitic neutrons needs extensive investigation, mainly in the part of the neutron fluence and the resulting fission reaction rate for each target, based on simulation results and the corresponding fission cross section of reference reactions as will be described below.

### *Neutron beam characterization*

During the irradiations, several parasitic reactions took place, affecting the monocromaticity of the neutron beam, resulting to the production of a low energy tail with some low energy distinct peaks, along with the main neutron energy. The monitoring of the parasitic neutrons was possible through a combination of both experimental (multiple foil activation) and simulation techniques (Monte Carlo simulations).

The main sources of the parasitic neutrons that have to be taken into consideration in the present work, resulted from reactions of

- ❖ Deuterons with nuclei present in the tritiated target itself
- ❖ Deuterons with nuclei present in the beam line (collimators, beam pipe etc.)
- ❖ Neutrons with materials existing in the experimental area (neutron scattering)

Regarding the target and the beam line, parasitic  $^{12}\text{C}(\text{d},\text{n})^{13}\text{N}$  and  $^{2}\text{H}(\text{d},\text{n})^{3}\text{He}$  reactions can occur due to carbon built up, and the implantation of deuteron nuclei in the target from previous irradiations, respectively. Since the target is not heavily used though, the main source of parasitic neutrons is expected to be the  $^{12}\text{C}(\text{d},\text{n})^{13}\text{N}$  reaction. Deuteron break-up in the field of  $^{3}\text{H}$  nuclei should also be taken into account when  $E_{\text{d}} > 3.7$  MeV. As far as the beam line is concerned, inevitable oxidation processes occur, resulting to the production of  $^{16}\text{O}$ , leading eventually in the  $^{16}\text{O}(\text{d},\text{n})^{17}\text{F}$  parasitic reaction, with a threshold of  $\sim 1.8$  MeV meaning that the contribution of this specific reaction will only be evident when  $E_{\text{d}} > 1.8$  MeV. Finally, neutron scattering is also possible from the materials existing in the experimental area and will be taken into account, along with the aforementioned sources of parasitic neutrons.

### *Simulations*

The production and the propagation of the neutron beam will be modeled via the NeuSDesc (Neutron Source Description) code [16] for each neutron energy, coupled with the SRIM (Stopping and Range of Ions in Matter) code that takes into consideration the energy loss, the energy and angular straggling of the deuteron beam within the target and the surrounding materials as well as the cross-section and kinematics of the  $^{3}\text{H}(\text{d},\text{n})$  reaction. The output of NeuSDesc can act as a source file for Monte Carlo simulations using the MCNP5[17] code and thus, the neutron energy spectrum and the fluence at the position of each target in the fission chamber can be estimated. The theoretical neutron fluence will be then used to estimate the theoretical reaction rate for the  $^{238}\text{U}$  target and then a statistical correction factor will be introduced to normalize the theoretical reaction rate to the experimental reaction rate, obtained from the experimental data.

Further Monte Carlo simulations will be performed, for the estimation of the low energy fission fragments that were rejected by the amplitude threshold. These simulations will be performed via the use of FLUKA[18] and GEF[19] codes. The latter is responsible for the generation of fission fragment distributions. It is noted, that the estimation of the amount of the fission fragments intercepted within the target is also possible with these simulations.

Detailed MCNP simulations have been also carried out to take into account the geometry corrections of the neutron flux among the different targets in the MicroMegas assembly. The results of the neutron flux from this process should be consistent in comparison with the experimental multiple foil activation method.

### *Multiple foil activation technique*

The experimental method for the compensation of the inevitable parasitic neutrons which accompany the main neutron beam, was the multiple foil activation technique, implementing Al, In, Nb and Au foils.

The  $^{115}\text{In}(\text{n},\text{n}')$  $^{115\text{m}}\text{In}$  reaction, with an energy threshold of  $>0.5\text{MeV}$ , will be used for the estimation of parasitic neutrons yielding from the  $^{12}\text{C}(\text{d},\text{n})^{13}\text{N}$  reaction since its cross-section is in the order of 0.3 b in the energy range between 0.693-3.65 MeV, while the non-threshold  $^{197}\text{Au}(\text{n},\gamma)^{198}\text{Au}$  reaction is more appropriate for the evaluation of the low energy neutrons produced by the  $^{16}\text{O}(\text{d},\text{n})^{17}\text{F}$ ,  $^{12}\text{C}(\text{d},\text{n})^{13}\text{N}$  reactions as well as from the scattered neutrons in the experimental area.

Finally, the  $^{27}\text{Al}(\text{n},\text{a})^{24}\text{Na}$ ,  $^{197}\text{Au}(\text{n},2\text{n})^{196}\text{Au}$ ,  $^{93}\text{Nb}(\text{n},2\text{n})^{92\text{m}}\text{Nb}$  reactions will be used for the estimation of the main energy peak due to their relatively high thresholds (3.2, 8.1 and 8.9 MeV, respectively). The flux in the actinide targets will be calculated with a correction geometrical factor due to the distance between the foils and the targets, as well as the kinematics of the neutron producing reaction. More information about the multiple foil activation technique regarding this work is described in [15].

The final flux results from the activation technique and the simulations, will then be compared to the results from the liquid scintillator spectra as well as from the parasitic neutrons produced from the bombardment of the Cu foil with the deuteron beams.

## SUMMARY

The measurements of the  $^{234}\text{U}(\text{n},\text{f})$ ,  $^{236}\text{U}(\text{n},\text{f})$  and  $^{232}\text{Th}(\text{n},\text{f})$  reactions have been successfully completed at neutron energies of 14.8, 15.2, 17.8 and 19.2 MeV and the analysis of the experimental data is ongoing. However, the first results are very promising towards a reliable calculation of the fission cross section in neutron energies above 15 MeV. The cross-sections of these reactions will be deduced, relative to the  $^{238}\text{U}(\text{n},\text{f})$  reference reaction. Monte Carlo simulations are also in progress implementing NeuSDesc and MCNP5 codes for an adequately precise reproduction of the neutron fluence, as well as the combined use of FLUKA and GEF codes for the simulation of the fission fragment and  $\alpha$ -particle detector efficiency.

## References

- [1] F. Tovesson *et al.*, Nucl. Sci. and Eng. 178, 57 (2014)
- [2] D. Karadimos *et al.*, Phys. Rev. C89, 044606 (2014)
- [3] C. Paradela *et al.*, Phys. Rev. C82, 0346601 (2010)
- [4] F. Manabe *et al.*, Fac. of Engineering, Tohoku Univ. Tech. Report 52, 97 (1988)
- [5] V.M.Pankratov *et al.*, Atomnaya Energiya 9, 399 (1960)
- [6] P.W.Lisowski *et al.*, Conf. on Nucl. Data For Sci. and Technol., 97 (1988)
- [7] P.F.Rago *et al.*, Health Physics 13, 654 (1967)
- [8] V.M.Pankratov, Atomnaya Energiya 14(2), 177 (1963)
- [9] D.A. Brown *et al.*, Nucl. Data Sheets 148, 1 (2018)
- [10] JEFF-3.3: Evaluated Data Library (2017), <http://www.oecd-nea.org/dbdata/jeff/jeff33/>
- [11] K. Shibata *et al.*, Nucl. Sci. Tech. 48, 1 (2011)
- [13] R. Vlastou *et al.*, Nucl.Instr.Meth. B269(2011)3266
- [14] R. Vlastou *et al.*, Proc. 24<sup>th</sup> HNPS Symposium p. 34 (2015)
- [15] V. Michalopoulou *et al.*, Proc. 26<sup>th</sup> HNPS Symposium p. 239 (2017)
- [16] “NeusSDesc – Neutron Source Description”, Evert Birgesson and Göran Lövestam, EUR 23794 EN – 2009
- [17] L. Waters *et al.*, AIP Conf. Proc. 896, 81 (2007)
- [18] “FLUKA: a multi-particle transport code”, A.Ferrari *et al.*, CERN-2005-10 (2005), INFN/TC\_05/11, SLAC-R-773
- [19] K.H. Schmidt *et al.*, Nucl. Data Sheets 131, 107 (2016)